Atmospheric
Chemistry
and Physics

Open Access

# Total ozone trends and variability during 1979–2012 from merged data sets of various satellites

**W. Chehade, M. Weber, and J. P. Burrows**

Institute of Environmental Physics (IUP), University of Bremen, Bremen, Germany

*Correspondence to:* W. Chehade (chehade@iup.physik.uni-bremen.de)

**Abstract.** The study presents a long-term statistical trend analysis of total ozone data sets obtained from various satellites. A multi-variate linear regression was applied to annual mean zonal mean data using various natural and anthropogenic explanatory variables that represent dynamical and chemical processes which modify global ozone distributions in a changing climate. The study investigated the magnitude and zonal distribution of the different atmospheric chemical and dynamical factors contributing to long-term total ozone changes. The regression model included the equivalent effective stratospheric chlorine (EESC), the 11-year solar cycle, the quasi-biennial oscillation (QBO), stratospheric aerosol loading describing the effects from major volcanic eruptions, the El Niño–Southern Oscillation (ENSO), the Arctic and Antarctic oscillation (AO/AAO), and accumulated eddy heat flux (EHF), the latter representing changes due to the Brewer–Dobson circulation. The total ozone column data set used here comprises the Solar Backscater Ultraviolet SBUV/SBUV-2 merged ozone data set (MOD) V8.6, the merged data set of the Solar Backscaterr Ultraviolet, the Total Ozone Mapping Spectrometer and the Ozone Monitoring Instrument SBUV/TOMS/OMI (1979–2012) MOD V8.0 and the merged data set of the Global Ozone Monitoring Experiment, the Scanning Imaging Absorption spectroMeter for Atmospheric ChartograpHY and the Global Ozone Monitoring Experiment 2 GOME/SCIAMACHY/GOME-2 (GSG) (1995–2012). The trend analysis was performed for twenty-six 5° wide latitude bands from 65° S to 65° N, and the analysis explained most of the ozone variability to within 70 to 90 %. The results show that QBO dominates the ozone variability in the tropics ($\pm 7$ DU) while at higher latitudes, the dynamical indices, AO/AAO and eddy heat flux, have substantial influence on total ozone variations by up to $\pm 10$ DU.

The contribution from volcanic aerosols is only prominent during the major eruption periods (El Chichón and Mt. Pinatubo), and together with the ENSO signal, is more evident in the Northern Hemisphere. The signature of the solar cycle covers all latitudes and contributes about 10 DU from solar maximum to solar minimum. EESC is found to be a main contributor to the long-term ozone decline and the trend changes after the end of the 1990s. From the EESC fits, statistically significant upward trends after 1997 were found in the extratropics, which points at the slowing of ozone decline and the onset of ozone recovery. The EESC based trends are compared with the trends obtained from the statistical piecewise linear trend (PWLT) model (known as hockey stick) with a turnaround in 1997 to examine the differences between both approaches. In case of the SBUV merged V8.6 data the EESC and PWLT trends before and after 1997 are in good agreement (within $2\sigma$), however, the positive post-1997 linear trends from the PWLT regression are not significant within $2\sigma$.

A sensitivity study is carried out by comparing the regression results, using SBUV/SBUV-2 MOD V8.6 merged time series (1979–2012) and a merged data set combining SBUV/SBUV-2 (1979–June 1995) and GOME/SCIAMACHY/GOME-2 ("GSG") WFDOAS (Weighting Function DOAS) (July 1995–2012) as well as SBUV/TOMS/OMI MOD V8.0 (1979–2012) in the regression analysis in order to investigate the uncertainty in the long-term trends due to different ozone data sets and data versions. Replacing the late SBUV/SBUV-2 merged data record with GSG data (unscaled and adjusted) leads to very similar results demonstrating the high consistency between satellite data sets. However, the comparison of the new SBUV/SBUV-2 MOD V8.6 with the MOD V8.0 and

MOD8.6/GSG data showed somewhat smaller sensitivities with regard to several proxies as well as the linear EESC trends. On the other hand, the PWLT trends after 1997 show some differences, however, within the $2\sigma$ error bars the PWLT trends agree with each other for all three data sets.

## 1 Introduction

Total ozone changes reflect changes in lower stratospheric ozone that are governed by chemical and dynamical short-term as well as long-term variability. Global ozone amounts decreased severely between the eighties and the mid-nineties, where they reached minimum values. This decline was mainly due to the impact of the uncontrolled anthropogenic emissions containing the halogens, chlorine and bromine (chlorofluorocarbons CFCs, halons), which depleted stratospheric ozone through catalytic chemistry. The chemical processes involving ozone depleting substances (ODSs), in particular the heterogeneous reactions in the polar region (ozone hole), are well known and documented in previous studies (e.g. Solomon, 1999; Staehelin et al., 2001) and various ozone assessments (World Meteorological Organization WMO (1999, 2003, 2007, 2011); Stratospheric Processes And their Role in Climate SPARC, 1998). The ODS emissions have been controlled by the implementation of the Montreal Protocol (1987) and its Amendments and Adjustments. Global ozone levels showed a slowing in the decline and started to increase starting in the mid-nineties in response to the phase out of ODSs in the stratosphere (WMO, 2003, 2007, 2011 and references therein). Some studies on the other hand have shown that variability of atmospheric dynamics on decadal time scales may also contribute to ozone trends (e.g. Hood and Soukharev, 2005; Reinsel et al., 2005; Dhomse et al., 2006; Wohltmann et al., 2007; Mäder et al., 2007). Long-term variability of stratospheric ozone is also seen to be influenced by variations in solar radiation (Chandra and McPeters, 1994; Bojkov and Fioletov, 1995; Miller et al., 1996; Zerefos et al., 1997; McCormack et al., 1997; Hood, 1997; Ziemke et al., 1997; Lee and Smith, 2003; Soukharev and Hood, 2006; Fioletov, 2009) and aerosols injected in the stratosphere after major volcanic eruptions (Hofmann and Solomon, 1989; Peter, 1997; Solomon, 1999).

Analysis of long-term changes in ozone in order to detect a statistically significant trend after the levelling off of the ODSs in the stratosphere requires the full understanding and proper accounting of all the processes contributing to ozone variability from interannual to decadal time scales. Global and long-term total ozone measurements acquired from various satellite-borne atmospheric chemistry sensors (multi-decadal data sets) are very useful for monitoring and studying ozone variability and for determining long-term global trends.

Previous trend assessments modelled the response of ODS related signal in terms of linear trends based on the expected linear increase and phasing out of ODSs. This statistical approximation of ODSs is well known as the piecewise linear trend (PWLT or hockey stick) model with a turnaround in the late 1990s, when the stratospheric halogens (released from ODSs) reached maximum. In this study we used multiple linear regression (MLR) which is a standard trend analysis tool to quantitatively asses the observed total ozone variations due to different natural and anthropogenic influences (WMO, 2003, 2007, 2011, and references therein), with the long-term trend in ozone related to ODSs described by the equivalent effective stratospheric chlorine function (EESC).

Steinbrecht et al. (2011) reported a 2 DU decade$^{-1}$ EESC-based 2000–2010 trend in annual mean total ozone measured by Dobson and Brewer spectrometers at the midlatitude station Hohenpeissenberg ($48°$ N, $11°$ E), while Nair et al. (2013) showed that the total column ozone trends estimated over 1997–2010 period measured at the northern Haute-Provence Observatory (OHP) midlatitude station ($43.9°$ N, $5.7°$ E) from Dobson and Système d'Analyse par Observation Zénithale spectrometers using the PWLT and EESC functions are about 6.5 and 4.2 DU decade$^{-1}$, respectively. Several other studies investigated ozone variability due to various dynamic processes (Rieder et al., 2010a, b, 2011, 2013; Frossard et al., 2013). Ziemke and Chandra (2012) found a turnaround in global stratospheric ozone column (mostly in the Northern Hemisphere) in the mid-nineties from the trend analysis of the 32 yr TOMS (Total Ozone Mapping Spectrometer) and OMI (Ozone Monitoring Instrument) record (1979–2010). They found trends of similar magnitudes but with opposite signs before 1993 and after 1996. Mäder et al. (2010) investigated MLR trends of total ozone form the Brewer and Dobson network up to 2008. They showed that for the majority of stations, the EESC term provides better fits than an MLR with a continuous linear trend up to the end of the data record. From this they concluded the success from the implementation by the Montreal Protocol and its amendments.

The aim of this paper is first to assess and update the global trends of total ozone using updated satellite data records up to the end of 2012. The trends are determined from a statistical analysis of thirty-four years of total ozone data. The estimated EESC-based trends are compared with the trends obtained from PWLT analysis to assess the differences between the models as the latter is sensitive to adding more data after the turnaround point. Moreover, the same statistical analysis is applied to different consolidated ozone data sets to investigate the uncertainty in the long-term trends due to the use of different ozone satellite data sets.

In Sect. 2, the major chemical and dynamical processes contributing to ozone variability are briefly summarized. The zonal mean total ozone data sets are described in Sect. 3, and the multiple linear regression model applied to the zonal total ozone data is presented in the following section. Section 5
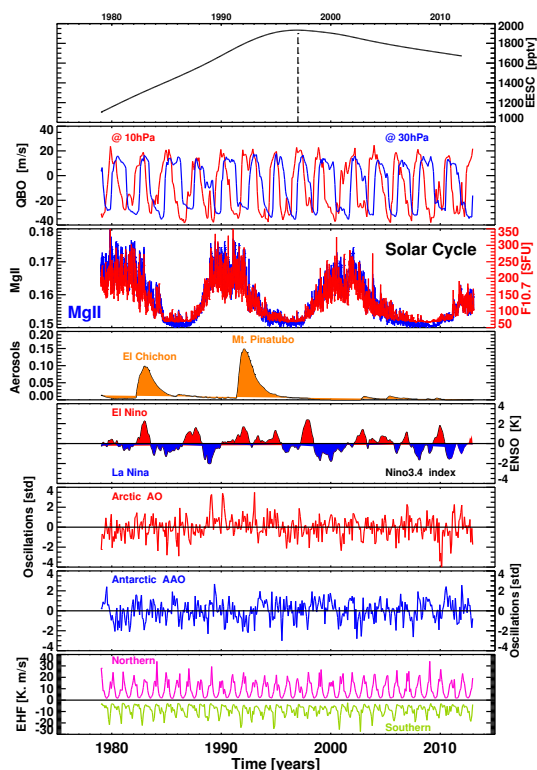
**Figure 1.** Time series of the different explanatory variables used in this study are displayed: stratospheric loading of ODSs (first panel) in terms of equivalent effective stratospheric chlorine (EESC) in pptv. Quasi-biennial oscillation (QBO) indices at 10 hPa (red) and at 30 hPa (blue) are shown in the second panel. The third panel displays the 11-year solar cycle as expressed by the solar flux at 10.7 cm (red) and core-to-wing ratio of the magnesium line MgII at 280 nm (blue). Time series of mean optical thickness at 550 nm (orange) to account for volcanic aerosol enhancements are presented in the fourth panel. Niño 3.4 Index describing the state of the El Niño/Southern Oscillation (ENSO) is shown in panel five: El Niño (red) and La Niña (blue). The next two panels show the teleconnection patterns: Arctic oscillation (AO) index in red and Antarctic oscillation (AAO) index in blue. In the last panel, extratropical eddy heat flux (EHF) at 100 hPa averaged over midlatitudes (area weighted between 45° N and 75° N) and averaged from October to March in the Northern Hemisphere (magenta) and from March to September in the Southern Hemisphere (green).

discusses the results in detail, and Sect. 6 discusses the ODS related trends from EESC and PWLT regressions. The sensitivity of using different ozone data sets in the regression are presented in Sect. 7, and the last section presents the major conclusions drawn.

## 2 Main contributors to ozone variability

The various proxies associated with natural and anthropogenic processes that describe the chemical and dynamical changes in total ozone in the MLR are shown in Fig. 1.

The different processes are briefly summarized below.

### 2.1 Brewer-Dobson circulation

Ozone is transported through the Brewer–Dobson circulation (BDC) in the lower to middle stratosphere that moves the upwelling air parcels from the tropics polewards, and then subsides in extratropics and high latitudes, where it builds up during wintertime. This meridional circulation is driven by planetary-scale atmospheric waves (Rossby and gravity waves) which are generated in the troposphere and propagated upwards to the stratosphere (Haynes et al., 1991; Rosenlof and Holton, 1993; Newman et al., 2001; Plumb, 2002). The influence of the meridional circulation in a given winter impacts the ozone variability well into spring and summer (Fioletov and Shepherd, 2003; Weber et al., 2011). The winter-accumulated lower-stratosphere eddy heat flux (EHF) is considered a good measure (proxy) of the interannual variability of ozone due to the BDC variations (Fusco and Salby, 1999; Newman et al., 2001; Randel and Stolarski, 2002; Dhomse et al., 2006; Weber et al., 2011).

The dominant recurrent non-seasonal sea level pressure variation pattern north/south of 20° S/N latitude known as the Arctic Oscillation (AO) and Antarctic Oscillation (AAO) also contribute to ozone fluctuations and can also be considered as a dynamical explanatory variable (Fusco and Salby, 1999; Hartmann et al., 2000; Appenzeller et al., 2000; Randel and Stolarski, 2002; Kiesewetter et al., 2010; Steinbrecht et al., 2011). Both the AO/AAO and the QBO phase modulate the wave propagation and relate to BDC variability (Baldwin et al., 2001).

### 2.2 Quasi-biennial oscillation (QBO)

The equatorial stratosphere is characterized by the slow recurring quasi-biennial oscillation (QBO) (Angell and Korshover, 1964) which influences the interannual variability of total ozone columns (Baldwin et al., 2001). A secondary meridional circulation by the QBO is induced and superimposed on the normal Brewer–Dobson circulation, which either enhances or weakens the BDC depending on the phase of QBO. The QBO signal also affects ozone variability at high latitudes (Bowman, 1989; Lait et al., 1989; Chandra and Stolarski, 1991) and even effects the distortion of wintertime stratospheric polar vortex by modulating the propagating extratropical wave flux or Eliassen–Palm flux (Dunkerton and Baldwin, 1991). This modulation is called the Holton–Tan effect (Holton and Tan, 1980) with its largest signal being in winter and spring (Tung and Yang, 1994; Randel and Cobb, 1994; Baldwin et al., 2001).

### 2.3 El Niño-Southern Oscillation (ENSO)

ENSO is the dominant source of interannual variability of tropical climate, it also impacts the chemistry of trace gases in the troposphere. During the 1997/8 El Niño event,

highest amounts of tropospheric column ozone (up to 25 DU increase) were registered in the tropics (Chandra et al., 1998; Fujiwara et al., 1999; Thompson et al., 2001), half of the increase resulted from El Niño-driven large scale changes in the ocean–atmosphere dynamics that transported ozone rich air from the stratosphere to the troposphere as reported by some modelling studies (e.g. Sudo and Takahashi, 2001; Chandra et al., 2002; Zeng and Pyle, 2005). Ziemke et al. (2010) even proposed a new El Niño index derived from tropical column ozone.

ENSO phases have a global impact, affecting the circulation in the extratropics by modulating the generation and propagation of Rossby waves which is strongly evident in the northern winter months (Trenberth et al., 2002). The warm phase is associated with stratospheric warming (van Loon and Labitzke, 1987; Labitzke and van Loon, 1999), and a strengthened BDC in the middle atmosphere yielding an enhanced upwelling of ozone-rich air from the tropics and a weaker polar vortex (Newman et al., 2001; Randel and Stolarski, 2002; Bronnimann et al., 2004; Manzini et al., 2006; Taguchi and Hartmann, 2006; Camp and Tung, 2007). ENSO results in temperature and ozone anomalies in the stratosphere that are opposite to the tropospheric anomalies.

### 2.4 Chlorine and bromine containing (ODSs)

The evolution of the long-lived ODSs is a key parameter to describe long-term ozone changes. Equivalent Effective Stratospheric Chlorine (EESC) index is used as a measure of the inorganic chlorine and bromine amounts accumulated in the stratosphere weighted by their ozone-destructive potential and fractional release rate (WMO, 1999, 2003, 2007, 2011). This is proportional to changes in total column ozone (Daniel et al., 1995). Stratospheric EESC is calculated from the surface measurements of tropospheric ODS abundances taking into account the greater per-atom potency of stratospheric bromine (Br) compared to chlorine (Cl) in its ozone destruction with a constant factor, $\alpha$ (EESC $= \mathrm{Cl} + \alpha \cdot \mathrm{Br}$), conversion of $\mathrm{Cl_y}$ and $\mathrm{Br_y}$, and the transit times (or ages) the air takes to be transported from surface to different regions in the stratosphere. The EESC index has already been used in several statistical models of ozone trends, (e.g. Newman et al., 2004; Fioletov and Shepherd, 2005; Dhomse et al., 2006; Stolarski and Frith, 2006; Randel, 2007; Harris et al., 2008; Kiesewetter et al., 2010).

### 2.5 Solar cycle

Solar variability is considered a dominant form of long-term ozone changes and has been included in all ozone trend assessments (WMO, 1999, 2003, 2007, 2011). Global total ozone amounts vary by 2 to 3 % in phase with the 11-year solar cycle (WMO, 2003, 2007). In relation to the 11-year solar cycle, a clear decadal response is detected in long-term ozone

records and is in phase with it (Chandra and McPeters, 1994; Bojkov and Fioletov, 1995; Miller et al., 1996; Zerefos et al., 1997; McCormack et al., 1997; Hood, 1997; Ziemke et al., 1997; Lee and Smith, 2003; Soukharev and Hood, 2006; Fioletov, 2009).

### 2.6 Aerosols

Major volcanic eruptions inject large amounts of sulfate aerosols into the stratosphere that perturb stratospheric temperature and circulation and enhance catalytic ozone depletion (Hofmann and Solomon, 1989; Peter, 1997; Solomon, 1999) by releasing chlorine and bromine from ODSs. The eruptions of the tropical volcanoes of El Chichón (Mexico, 1982) and Mt. Pinatubo (Philippines, 1991) were the major volcanic activities since the late 1970s. Stratospheric ozone reduced significantly following the eruptions in the Northern Hemisphere (Randel et al., 1995; Solomon et al., 1996; SPARC, 1998; WMO, 1999, 2003, 2007, 2011) which persisted for two to three years, while Southern Hemisphere ozone records did not show any pronounced ozone deficit (Fioletov et al., 2002; WMO, 2003, 2007, 2011). Several studies (Schnadt Poberaj et al., 2011; Aquila et al., 2013) showed that enhanced ozone transport through changes in dynamical processes counteracted the chemical losses.

### 3 Satellite total ozone time series

Zonal mean total ozone columns from the Solar Backscatter Ultraviolet (SBUV/SBUV-2) Merged Ozone Data Set (MOD) Version 8.6 spanning from 1979 to 2012 (Frith et al., 2012), were used in this study. MOD V8.6 is constructed by combining the homogenized records from the Nimbus 7 SBUV instrument and series of SBUV(/2) instruments on the National Oceanic and Atmospheric Administration (NOAA) satellites (NOAA's 9, 11, 14, 16, 17, 18, and 19), the construction of the MOD V8.6 is based on the calibration and analysis processes including a detailed analysis of instrumental uncertainties and presented in DeLand et al. (2012), Bhartia et al. (2013) and McPeters et al. (2013). For the sensitivity study, the TOMS/SBUV/OMI Version 8.0 ozone data product (1979–2012) were also used. This data set combines data from eight independent backscatter ultraviolet technique (BUV-type) satellite instruments, Total Ozone Mapping Spectrometer (TOMS), SBUV/SBUV-2, and Ozone Monitoring Instrument (OMI). Drifts and biases in overlapping periods among instruments were removed (Stolarski and Frith, 2006). The MOD V8.0 is based upon data that have been retrieved using the TOMS V8.0 column algorithm, while the MOD V8.6 is solely based on SBUV/SVUV-2 data and the SBUV V8.6 retrieval algorithm, which obtains column amounts from integrated profiles (Bhartia et al., 2013). Both MOD V8.0 and V8.6 can be obtained from http://acd-ext.gsfc.nasa.gov/Data_services/merged/.

In this study we also used the merged total ozone merged data from the Global Ozone Monitoring Experiment, the Scanning Imaging Absorption spectroMeter for Atmospheric ChartograpHY and the Global Ozone Monitoring Experiment 2 GOME/SCIAMACHY/GOME-2 (GSG). The total ozone retrieval is carried out using the weighting function differential optical absorption spectroscopy (WFDOAS) algorithm (Coldewey-Egbers et al., 2005). This data set extends from 1995 to 2012 and combines data from GOME (1995–2003) (Coldewey-Egbers et al., 2005; Weber et al., 2005), SCIAMACHY (2002–2006) (Bracher et al., 2005) and GOME-2 (2007–present) (Weber et al., 2007). GOME was very stable over the operational period (1995–2012) and selected as a reference for bias adjusting SCIAMACHY and GOME-2 data (Kiesewetter et al., 2010; Weber et al., 2011, 2013). Adjustments were made by determining latitude-dependent scaling factors (GOME-2 and SCIAMACHY) from the monthly mean zonal mean ozone ratio with respect to GOME. The data can be obtained from http://www.iup.uni-bremen.de/gome/wfdoas/merged/.

Figure 2 shows annual means of the area-weighted total ozone columns over the period 1979–2012 of the different global data sets used in this study and the ground-based measurements which combines Brewer, Dobson, and filter spectrometer data for various zonal bands: global (60° S–60° N), middle latitudes in both hemispheres (35–60°) and the tropics (25° S–25° N), respectively. The observed total column ozone values are currently 2 % lower than the 1964–1980 total ozone columns on a global scale, about −4 % in the Northern Hemisphere (35–60° N) and about −7 % in the Southern Hemisphere (35–60° S) while in the tropics (25° S–25° N) total column are almost unchanged.

The SBUV MOD V8.6 ozone columns are consistent with about 1 % when compared to ground based data from Brewer and Dobson spectrophotometers (McPeters et al., 2013). The TOMS/SBUV/OMI V8.0 ozone zonal average data are mostly 1–2 % higher than MOD V8.6 data. The WFDOAS GSG data set shows very good agreement (within 1 %) with ground-based data and with other satellite data (Weber et al., 2005; Fioletov et al., 2008; Koukouli et al., 2012; Lerot et al., 2013; McPeters et al., 2013; Weber et al., 2013) including SBUV/SBUV-2 MOD V8.6 data set and the GOME-Type total ozone record (GTO) from the three European sensors based on the DOAS approach using products obtained with the GOME Data Processor (GDP5/GODFIT) (Van Roozendael et al., 2006; Loyola and Coldewey-Egbers, 2012; Lerot et al., 2013).
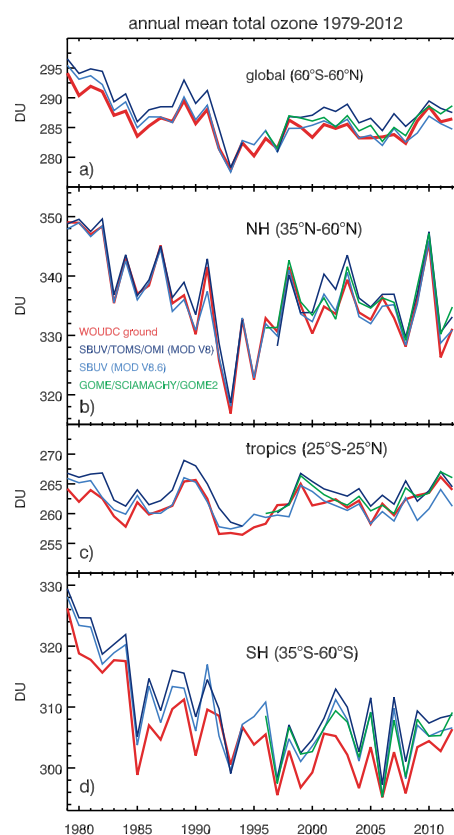


**Figure 2.** Annual mean area-weighted total ozone time series of ground-based measurements combining Brewer, Dobson, and filter spectrometer data (red, (Fioletov et al., 2002, 2008)), the merged SBUV/TOMS/OMI MOD V8.0 (dark blue: (Stolarski and Frith, 2006)), the merged SBUV/SBUV-2 MOD V8.6 (blue: DeLand et al. (2012); McPeters et al. (2013)), and GOME/SCIAMACHY/GOME-2 "GSG" (green, (Kiesewetter et al., 2010; Weber et al., 2011, 2013)), in the zonal bands: **(a)** 60° S–60° N (global), **(b)** 30–60° N (NH), **(c)** 25° S–25° N (tropics), and **(d)** 35–60° S (SH) zonal bands.

## 4 Multivariate linear regression

Trends in global total ozone are investigated through a multivariate linear regression model consisting of various explanatory parameters (as discussed above) which account for chemical and dynamical processes in the atmosphere. This statistical method has been frequently used in ozone assessments (Bojkov et al. (1990); SPARC (1998); CCM-Val (2010); WMO (1999, 2003, 2007, 2011) and references therein) in order to assess the contributions of various natural and anthropogenic changes to long-term and short-term variability of ozone. The annual mean total ozone column (TOZ) time series is constructed as a simple linear sum of explanatory-variable time series as follows:

$$
\begin{aligned}
\mathrm{TOZ}(n) = \quad & \mathrm{TOZ(n)^\circ} + \alpha^{\mathrm{EESC}} \cdot \mathrm{EESC}(n) \\
+ \quad & \alpha^{\mathrm{qbo}}_{10} \cdot \mathrm{qbo}_{10}(n) + \alpha^{\mathrm{qbo}}_{30} \cdot \mathrm{qbo}_{30}(n) \\
+ \quad & \alpha^{\mathrm{solar}} \cdot \mathrm{solar}(n) \\
+ \quad & \alpha^{\mathrm{aer}} \cdot \mathrm{aer}(n) \\
+ \quad & \alpha^{\mathrm{ENSO}} \cdot \mathrm{ENSO}(n) \\
+ \quad & \alpha^{\mathrm{AO/AAO}} \cdot \mathrm{AO/AAO}(n) \\
+ \quad & \alpha^{\mathrm{EHF}} \cdot \mathrm{EHF}(n) \\
+ \quad & \varepsilon(n), \quad\quad (1)
\end{aligned}
$$

where $n$ is a running index (from zero to 34) corresponding to all years during the period 1979–2012 while $\alpha^X$ represent the time dependent regression coefficients of each proxy ($X$) and $\varepsilon$ is the residual or noise time series. The EESC concentration was obtained from NASA Goddard Space Flight Center web site (http://acdb-ext.gsfc.nasa.gov/Data_services/automailer/index.html) and was calculated for a mean age of air of three years and width of age-of-air distribution of one and half years (Newman et al., 2006, 2007) and bromine efficiency of $\alpha = 60$ was used (Sinnhuber et al., 2009). Equatorial zonal winds at 10 and 30 hPa pressure levels (from FU Berlin, http://www.geo.fu-berlin.de/en/met/ag/strat/produkte/qbo/index.html) were used to provide the QBO index in the regression analysis. QBO at 10 and 30 hPa are out of phase ($\sim \pi/2$, Bojkov and Fioletov (1995); Steinbrecht et al. (2003)) and account for the effect of QBO strength and phase on ozone at different latitudes. This obviates the need to find the optimal time lag (Bojkov et al., 1990).

To account for volcanic aerosols after El Chichón and Mount Pinatubo eruptions, time dependent stratospheric aerosol optical depth (OD) at 550 nm (Sato et al., 1993) is used. The optical depth (http://data.giss.nasa.gov/modelforce/strataer/) is multiplied by the stratospheric chlorine content (EESC) (Wohltmann et al., 2007). To investigate the impact of UV solar irradiance modulation related to the 11-year solar cycle, core-to-wing ratio of the MgII line at 280 nm (http://www.iup.uni-bremen.de/gome/solar/MgII_composite.dat) is used as a proxy. There is no change in the fitting results when using the F10.7 cm solar radio flux alternatively. For the El Niño Southern Oscillation phenomenon, the Niño 3.4 index (http://www.cpc.ncep.noaa.gov/data/indices/ersst3b.nino.mth.81-10.ascii) is included in the regression. The AO/AAO index is obtained from NOAA National Weather Service Climate Prediction Center web site (http://www.cpc.ncep.noaa.gov/products/precip/CWlink/daily_ao_index/teleconnections.shtml) and the extratropical 100 hPa eddy heat flux (EHF) averaged over midlatitudes between 45° and 75° in each hemisphere is obtained from the European Centre of Medium Range Weather Forecasts (ECMRWF) ERA-Interim as described by Weber et al. (2011).

The residual circulation transports more stratospheric ozone in winter and the wintertime ozone anomalies remain evident till autumn. Weber et al. (2011) reported positive correlation between spring-to-fall ozone ratio and the winter mean eddy heat flux above and below 50° S/N, while in the tropics (till 40° S/N) the relation is anti-correlated. To account for ozone wintertime build up and its persistence through the summer, winter mean of AO/AAO and eddy heat flux indices (from October of the previous year until March for the Northern Hemisphere (NH) and April to September, for the Southern Hemisphere (SH)) are used. For the other proxies, the annual mean data obtained by averaging monthly mean values are used with no time lags.

The explanatory-variable time series used in a multivariate linear trend analysis must be fully independent (uncorrelated); in this study the correlations between predictors are very small (reaching a maximum of 0.3). In order to account for auto-regression, a Cochrane–Orcutt transformation (Cochrane and Orcutt, 1949) is applied to the regression. The transformation does not change the estimates of the fitting coefficients, however, the fitting errors increase due to the reduction in degree of freedom.

## 5 Results

The regression analysis (Eq. 1) is applied to SBUV/SBUV-2 Version 8.6 annual mean zonal mean total ozone data from 65° S to 65° N in steps of 5°. An example of the model and the contributions (in Dobson units, DU) of the different natural as well as anthropogenic explanatory variables are illustrated in Fig. 3 for the 60–65° N latitude band. The regressed ozone time series (blue, first panel) fits well to the ozone measurements (red) and follows the general features capturing the decline of ozone to the mid-1990s, the pronounced ozone losses after the Mt. Pinatubo eruption and the slow increase after that. The black curve (EESC) describes long-term variations attributed to anthropogenic emissions of ODSs. After 1997, a small increase ($3.65\pm0.8\,\mathrm{DU\,decade^{-1}}$) is attributed to the EESC decline. The regression fit shows that the the coefficient of determination, i.e $R^2$ (the ratio of the variance of all terms in Eq. 1 to the total variance), is 0.80, this implies that about 80 % of the observed variance of total ozone column can be explained by the regression. The residual mean square (rms, the sample estimate of the variance of the regression residuals) is 5.4 DU.

The green line in the second panel displays the regression residuals between measured and regressed data (in percent). The fitted signal of each explanatory parameter $\alpha^X \cdot X$ is shown in the third to seventh panel of Fig. 3. The overall combined QBO related component (black, $\alpha^{\mathrm{qbo}_{10}} \cdot \mathrm{qbo}_{10} + \alpha^{\mathrm{qbo}_{30}} \cdot \mathrm{qbo}_{30}$) contributes to interannual ozone variability, the fluctuation from easterly to westerly QBO phase at 10 hPa (red) and 30 hPa (blue) amounts to about 10 DU. The 11-year solar cycle contribution (blue, MgII index) reaches about
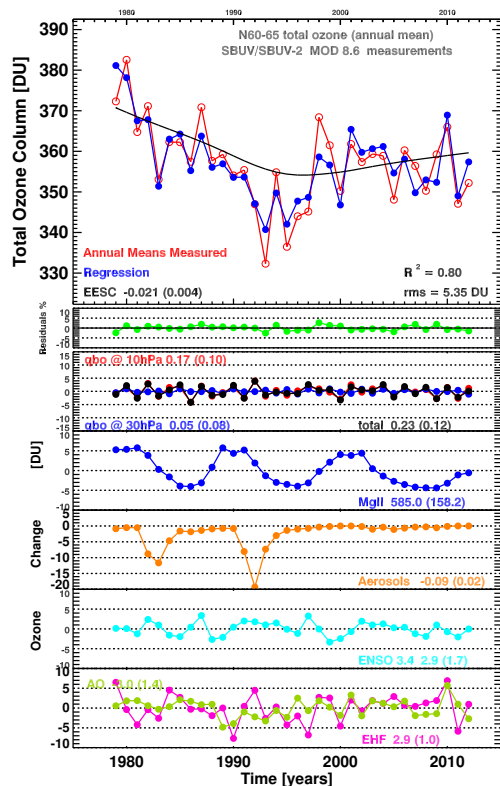
**Figure 3.** Annual mean total ozone variations for 60–65° N in DU (SBUV/SBUV-2 Version 8.6 data set from 1979–2012) and magnitude of contributing factors obtained by multiple linear regressions. Top panel: observed total annual mean data (red), corresponding fit (blue) and the EESC curve (black). Green line marks the residuals between the observed ozone and regressed time series (second panel). Bottom panels show the contributions from: QBO at 10 hPa (red), at 30 hPa (blue) and combined effect (black), blue: 11-year solar cycle (MgII index); orange: enhanced stratospheric aerosols; turquoise: ENSO (3.4) index, eddy heat flux in magenta and AO/AAO oscillation in lime-green, respectively. The coefficient of determination ($R^2$) between the observed and regressed ozone and root mean square (rms) are indicated in the first panel. The regression coefficients of various proxies along with the 1-$\sigma$ standard deviation (in brackets) are also indicated in each panel.



**Figure 4.** (top panel) $R^2$ and rms calculated from multiple linear regression of 1979–2012 merged SBUV/SBUV-2 Version 8.6 annual mean total ozone from 65° S to 65° N (results based on regression Eq. 1). The fitting coefficients of the different explanatory variables used in this study for each latitude band are displayed in respective colours as in Fig. 3. Error bars indicate the statistical significance at two sigma level.

10 DU from solar minimum to solar maximum. The aerosol response associated with El Chichón and Mount Pinatubo eruptions (orange) accounts for about 12 DU and 19 DU loss in total ozone in 1983 and 1992, respectively. The influence of ENSO (turquoise) is typically about ±4 DU, whereas the 1997/8 El Niño event contributed up to +3 DU. The highest contribution to total ozone variability arises from the dynamical explanatory variables (Eddy heat flux (magenta) and the negative and positive phases of AO/AAO (lime-green)) reaching about 12 DU. Both dynamical proxies were included in the analysis as the regression model worked better and improved the correlation and the coefficient of determination (not shown here). The regression coefficients of the
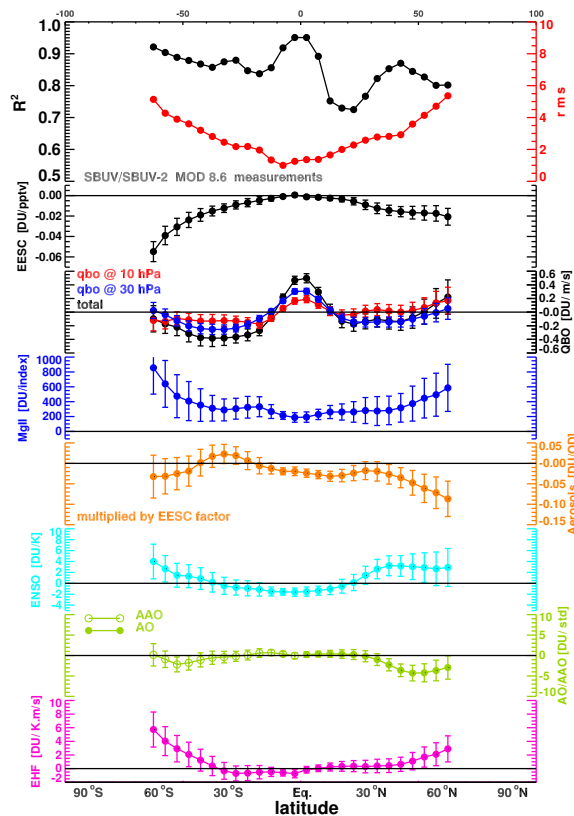
various proxies along with the standard deviation (in brackets) are noted as well in the plot.

Figure 4 shows the estimates of fitting coefficients of the different explanatory variables and the effect of each proxy on the interannual variability of total ozone measurements (using the same colour notation as in Fig. 3) for each latitude band. The top panel displays the coefficient of determination between measured annual ozone and regression results. Typical values are higher than 0.72 across all latitude bands showing that the statistical model explains the major part of the total ozone variance, in the tropics (within 5° S/N) the regression describes the total ozone variations almost completely. The values of the coefficients of determination in the Northern Hemisphere are less than those of its southern counterpart due to the larger variability in the Northern Hemisphere.

The second panel of Fig. 4 shows the total ozone response related to ODS abundance in the selected latitude bands as represented by the EESC term. The EESC coefficient increases in magnitude with increasing latitude. In the inner tropics the EESC trends are zero. The EESC response is

larger in the Southern Hemisphere as compared to the same latitudes in the Northern Hemisphere latitudes. The largest ozone loss attributed to the chemical ozone depletion by the accumulated anthropogenic ODSs are found south of 50° S in the "ozone hole" region. This indicates that the Antarctic ozone loss has a high impact on the long-term decline at Southern Hemisphere midlatitudes (Chipperfield, 2003; Fioletov and Shepherd, 2005; Kiesewetter et al., 2010). The error bars indicate the statistical significance at two sigma level (95 % significance level). The EESC term is statistically significant in all latitude bands except the tropics (20° S–20° N).

The total QBO coefficient, shown in black in the third panel, is symmetric about the equator in the tropics and changes sign at about 15° latitude. It dominates ozone variability in the tropical and southern subtropical regions with highest and clear influence between 5° S and 5° N while it is insignificant in the northern subtropics. Not unexpected, the 30 hPa QBO term dominates over the 10 hPa QBO term. The QBO phase change from the equator to the subtropics are due to a secondary circulation with the downward branch in the tropics and the upwelling branch in the subtropics (positive ozone anomalies in the tropics and negative in the 20–50° subtropical regions).

The solar coefficients are statistically significant at all latitudes. The coefficients of stratospheric aerosols (orange) in the fifth panel, are mostly negative and increases with increasing northern latitudes. El Chichón and Mt. Pinatubo eruptions significantly influence total ozone over the northern latitudes and the negative ozone signal is in good agreement with results reported in previous studies (Staehelin et al., 1998; Fioletov et al., 2002; Mäder et al., 2007; Wohltmann et al., 2007; Harris et al., 2008; Rieder et al., 2010a, b, 2011; WMO, 2007, 2011). At southern midlatitudes the signal is unexpectedly positive. Similar results were noted by (Fioletov et al., 2002) and were also documented in the WMO reports (WMO, 2003, 2007, 2011). This spatial pattern emanates from the dynamical processes in which enhanced ozone transport to southern midlatitudes driven by a strong warm ENSO phase and negative AAO accompanied by the shifting and stretching of the vortex towards the Antarctic Peninsula suppressed the ozone signal (Schnadt Poberaj et al., 2011; Aquila et al., 2013; Rieder et al., 2013).

The sixth panel shows the distribution of the ENSO coefficient over the studied latitude range. A significant moderate negative influence on total ozone is centered over the tropical region (15° S–10° N). The positive patterns in the northern high latitudes are interpreted as consequences of enhanced transport from the tropics during warm ENSO events (Frossard et al., 2013; Rieder et al., 2013) while the coefficients are statistically insignificant towards southern high latitudes (up to 55° S).

The AO estimates are found to be significant over the northern latitudes (35–60° N). Negative AO anomalies lead to enhanced ozone in the northern extratropics. The ex-
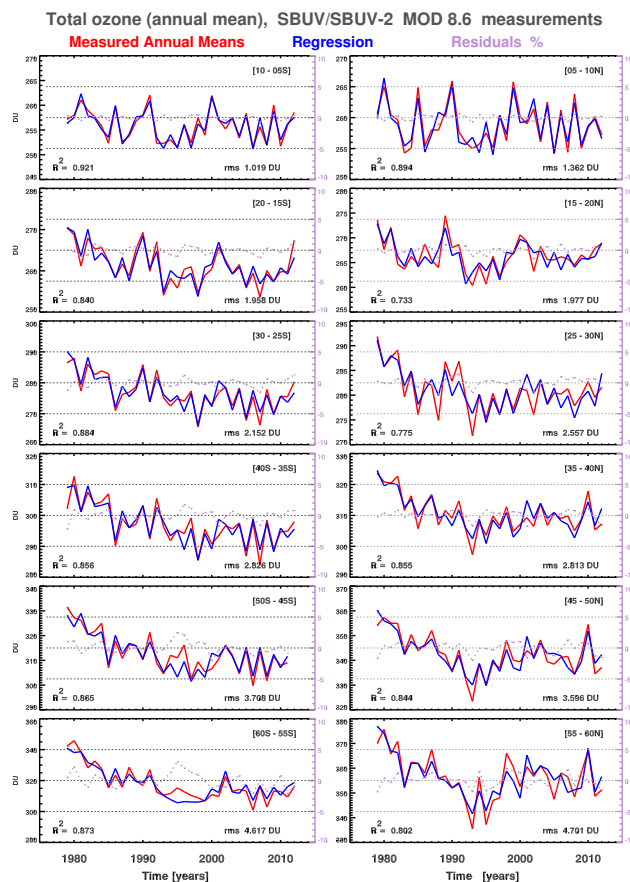


**Figure 5.** Observed SBUV/SBUV-2 V8.6 (red) annual zonal mean total ozone columns for selected latitude bands from 65° S to 65° N and regressed (blue) ozone obtained from regression models. The right hand scale in each panel gives the residuals in percent (violet). $R^2$ and rms are also noted for each latitude band.

tremely negative AO index in 2010 resulted in very high ozone throughout the northern extratropics (Steinbrecht et al., 2011). Similar to the NH, the negative AAO phases enhances SH ozone transport, however, the AAO contribution at high southern latitudes in the regression is statistically not significant except for the 45–55° S zonal band.

The winter mean eddy heat coefficients are statistically significant and dominate ozone variability in both hemispheres above 50° latitude.

The measured and modelled ozone are displayed in Fig. 5 for selected latitude bands. The reconstructed ozone generally captures the temporal ozone variations and follows the general features of the slow decline till the mid-nineties and the increase after that. The residuals (violet, right scale of the panels) are typically within 3 %. $R^2$, and rms are also displayed for each latitude band.

## 6  ODS related trends in ozone total column

Ozone trends related to ODSs are calculated for all latitude bands according to the full regression model (Eq. 1). Based on the EESC curves, two clear linear trends can be estimated. A decline in ozone amounts starts at the beginning of the measurements due to the increases in stratospheric ODS loading ($0.447\,\mathrm{ppbv\,decade^{-1}}$) until the turnaround of the ODS levels in 1997 (EESC maximum), and a negative trend following the levelling-off and phase out of ODSs in the stratosphere ($-0.179\,\mathrm{ppbv\,decade^{-1}}$) accompanied with an increase in total column levels. Both phases of the ODS related ozone trends can be approximated as the slopes of the declining and increasing phases of EESC multiplied by the EESC coefficient [DU decades$^{-1}$].

The pre-1997 and post-1997 EESC based linear trends (red solid circles) as a function of latitude are displayed in the bottom panel of Fig. 6. The positive trends after 1997 increase in magnitude with latitude and are statistically significant across nearly all latitude bands except the tropics (20° S–20° N). In the northern subtropics and extratropics, the positive trends are smaller than those in southern counterparts. This can be explained by the large dynamically driven variations dominating the ozone variability in northern latitudes (Reinsel et al., 2005; Dhomse et al., 2006; Wohltmann et al., 2007; Harris et al., 2008). The statistically significant trends after 1997 can, therefore, be attributed to the onset of anthropogenic (or ODS related) ozone recovery.

The ozone trends before and after the ODS turnaround can also be described by calculating piecewise linear trends (PWLT or hockey stick) (Reinsel et al., 2002, 2005; Newchurch et al., 2003; Miller et al., 2006; Vyushin et al., 2007, 2010; Yang et al., 2009). The PWLT model replaces the EESC term ($\alpha^{\mathrm{EESC}} \cdot \mathrm{EESC}(n)$) in Eq. 1 by two separate linear trend terms:

$$\alpha^{\mathrm{EESC}} \cdot \mathrm{EESC}(n) = \alpha^{t1} \cdot \delta(\leq 1997) + \alpha^{t2} \cdot \delta(> 1997),$$
(2)

where $\delta(\leq 1997)$ is a quantity corresponding to the years before 1997 subtracted from 1997 and zero after 1997 while $\delta(> 1997)$ is 0 before 1997 and 1997 subtracted from the years after 1997.

As for the EESC regression, the results obtained from the PWLT model (not shown here) showed the same patterns as in Fig. 5 with the coefficient of determination better than 0.72, the contributions of the other explanatory variables slightly altered. The MgII coefficient decreased by 10–30 % south of 35° S, the eddy heat flux coefficient slightly increased by 10 % in the same latitude bands while the aerosol signals dropped greatly in the same bands (statistically significant between 45° S and 60° S) when PWLT is used. The significant changes of the aerosols and MgII contributions are due to the evolution of the parameterited EESC in which the turnaround of ODS abundances starts in the early nineties and lasts till the late nineties (slow turnaround) peaking in
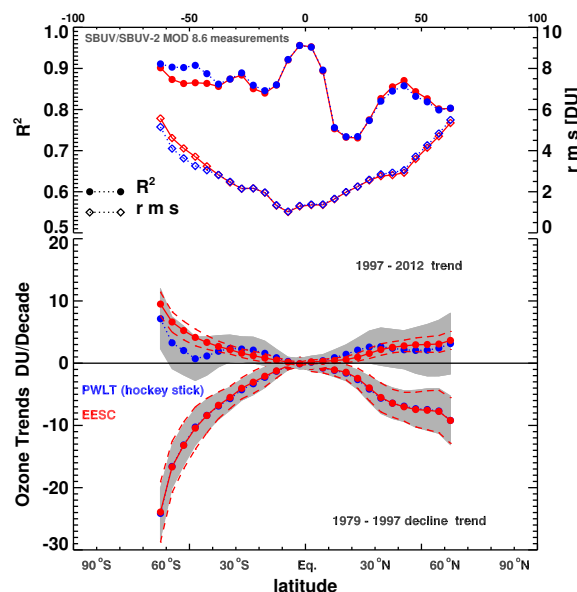


**Figure 6.** (top panel) Zonal distribution of $R^2$ and rms estimated for the 1979–2012 SBUV/SBUV-2 V8.6 merged data set from regression model based on Eq. (1) in red and the piecewise linear trend (PWLT or hockey stick) model in blue. (bottom panel) Zonal distribution of the linear trend of ozone in DU decade$^{-1}$ units calculated for the declining part of EESC during 1979–1997 and for the increasing part of EESC during 1997–2012 (red) as well as the trends before and after the ODS turnaround (1997) calculated by the PWLT model (blue). The statistical significance at two sigma level is indicated as grey shades for PWLT and dashed lines for EESC.

1997 compared to the sharp inversion of the ODS abundances used in the PWLT regression model. The aerosol signals of El Chichón and Mount Pinatubo are screened and picked up by ODS signal modelled by EESC which also influence the magnitude of the MgII signal. A brief explanation is given in the supplementary material.

Both of the above mentioned approaches equally well describe the total ozone changes during the last thirty years. Both EESC and PWLT related trends before and after 1979 are shown in Fig. 6. The fit is almost identical in the 35° S–65° N latitude range, as evident from the rms and coefficient of determination. Above 35° S, the PWLT fits provide lower residuals than the EESC fits. In this region, the PWLT trends after 1997 differ more strongly from the EESC trends as discussed further down.

Both EESC and PWLT based trends before 1997 are very close to each other and agree within the 2-sigma error bars (grey shades for PWLT and dashed lines for EESC). On the other hand, the positive trends after 1997 are also close to each other, the values of the PWLT trend dropped significantly south of 40° S. Moreover, the positive PWLT is statistically insignificant over the latitude bands except for the narrow band 20–30° in each hemisphere. The post-1997 PWLT trend in the southern high latitudes are up to four times less

than the EESC based trend but agree within the 95% error bars. The PWLT trend values after 1997 are different than expected and cannot be accounted as a full true response to the ODS decline after 1997 since PWLT regression analysis is very sensitive to the length of the data record after 1997 (Vyushin et al., 2010) or may contain contributions from other processes than ODSs. As the ODS related upward trend is fairly small, the PWLT is more strongly affected by uncertainties in the short-term variability.

## 7 Sensitivity of the trends acquired from different satellite ozone data records

In this study, the merged WFDOAS GOME/SCIAMACHY/GOME-2 (GSG, 1995–2012) zonal mean total ozone mean data set (Kiesewetter et al., 2010; Weber et al., 2011, 2013) and the TOMS/SBUV/OMI Version 8.0 (MOD8.0) ozone data product (1979–2012) (Stolarski and Frith, 2006) were also analysed using the regression model (Eq. 1) to investigate the uncertainty in long-term trends due to the use of different ozone data sets. The statistical analysis was applied for the same latitude range (65° S–65° N). The GSG data (July 1995–December 2012) was combined with SBUV/SBUV-2 merged V8.6 data (January 1979–June 1995) without adjustments of the GSG data. The results as a function of latitude are depicted in Figs. 7 and 8 together with the results for the TOMS/SBUV/OMI Version 8.0 data set and the previous results for the SBUV/SBUV-2 MOD V8.6 merged data (1979–2012). Both data sets are generally in good agreement with the SBUV/SBUV-2 merged V8.6 results. For the MOD8.6/GSG data in comparison to MOD V8.6, the determination coefficient are close at higher latitudes but decrease in the tropics and subtropics. The MOD8.6/GSG rms's are slightly higher within 15° S–15° N and almost unchanged elsewhere. The differences when replacing part of the MOD V8.6 data with GSG data are very small indicating excellent agreement between both data sets. On the other hand, the determination coefficient as well as rms for MOD V8.0 data improved between the 30° S and 60° S latitude range while north of 25° S the values dropped.

The fit coefficients of the MOD8.6/GSG and MOD V8.0 data follow the same pattern as that for the MOD V8.6 merged data set and agree within 2-sigma (see Fig. 8). The EESC signals and trends, QBO and aerosols estimates agree well and are within ±15 % with MOD V8.6 estimates. The other signals are significantly altered by the use of the GSG and MOD V8.0 data. The dynamical signals (ENSO, AO/AAO and EHF) obtained from MOD V8.0 regression analysis increased about 15–35 % north of 35° N, while MOD8.6/GSG data analysis revealed that the same signals are almost unchanged. The solar cycle contributions agree for MOD8.6/GSG and MOD V8.6, but MOD V8.0 show larger contributions in the Northern Hemisphere, but all data sets agree within their error bars.
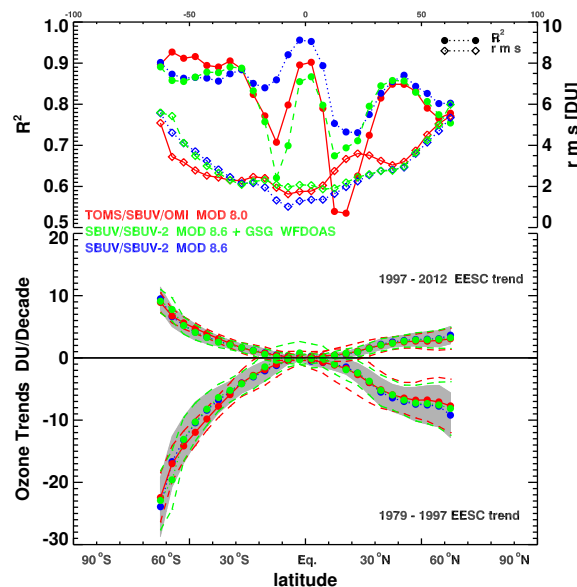


**Figure 7.** (top panel) Zonal distribution of $R^2$ and rms estimated for the merged GSG data (July 1995–December 2012) combined with SBUV/SBUV-2 MOD V8.6 data (January 1979–June 1995) displayed in green, SBUV/SBUV-2 MOD V8.6 ozone data (1979–2012) in blue and TOMS/SBUV/OMI MOD V8.0 merged data (1979–2012) in red. The results refer to analysis based on regression Eq. (1). (bottom panel) The EESC-based trends representing the decline from 1979 till 1997 (negative values) and and increase after 1997 (positive values) are displayed for all ozone data sets. Grey shades indicate the statistical significance at two sigma level for SBUV/SBUV-2 MOD V8.6, red dashed lines for TOMS/SBUV/OMI MOD V8.0 and green dashed lines for the SBUV/SBUV-2 MOD V8.6 + GSG WFDOAS data set.

As shown in Fig. 8, within $2\sigma$ all fitting coefficients agree with each other for all three data sets. In particular, the EESC trends are almost identical. This means that the GSG, MOD V8.0 and MOD V8.6 data sets are highly consistent.

However, there are some differences in the PWLT trends after 1997 between the three data sets as shown in Fig. 9. The post-1997 PWLT trends for the MOD V8.0 data are higher than those for MOD V8.6 and are statistically significant (95 % confidence). The post-1997 PWLT trends from MOD8.6/GSG data set lie somewhere between the SBUV merged MOD V8.6 and MOD V8.0. Both MOD V8.0 and MOD8.6/GSG show positive trends in the tropics after 1997 that are barely statistically significant. Within the combined error bars the PWLT trends agree between all data sets and at all latitudes. The EESC and PWLT trends before 1997 for each data set agree with each other for all three data sets. After 1997, there are some differences. For most latitudes the MOD V8.0 PWLT trends are larger than their respective EESC trends, while they agree for the MOD V8.6 data as mentioned before. An exception are the high southern latitudes where the MOD V8.0 show better agreement between PWLT and EESC, while larger differences are observed
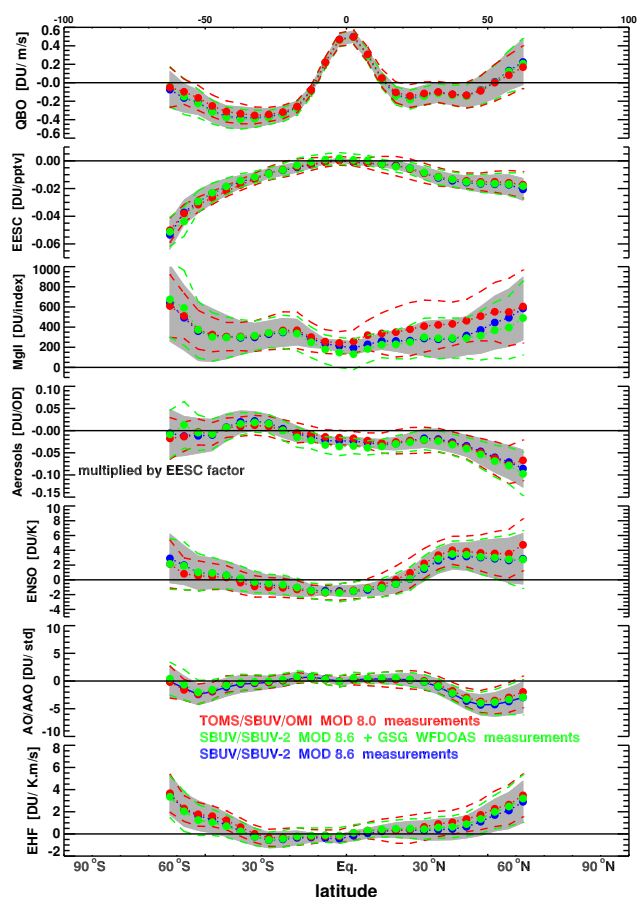
**Figure 8.** The fitting coefficients of the different explanatory variables used in the regression analysis of the different merged data sets. The statistical significance at two sigma level is displayed in respective colours as in Fig. 7.

for MOD V8.6. The MOD8.6/GSG trends form EESC and PWLT fits agree for most latitudes except for the positive PWLT trends after 1997 not seen in the EESC trend.

Within the $2\sigma$ error bars the PWLT trends agree with each other for all three data sets.

## 8   Summary and conclusions

In this study, long-term evolution of zonal mean annual mean total ozone measurements from merged data sets of various satellites over the period 1979–2012 between 65° S and 65° N were analysed by multiple linear regression. The regression analysis included different explanatory variables representing dynamical and chemical processes that modify global ozone distributions such as QBO, solar cycle, aerosols, ENSO, eddy heat flux, AO/AAO and the EESC terms. The SBUV/SBUV-2 merged data V8.6 (MOD V8.6) were analysed first. The regression model explained about 70–95 % of the ozone variability across the considered latitude range. The QBO signal dominates the tropical region
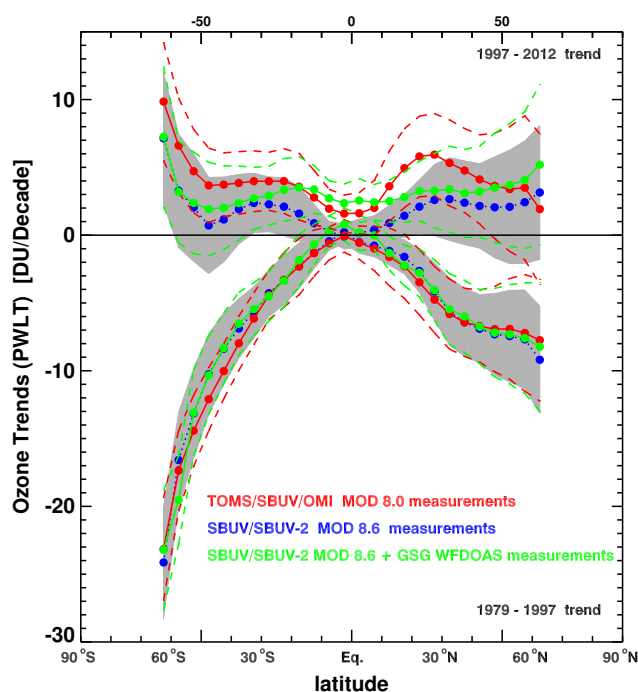


**Figure 9.** Comparisons between PWLT trends before and after 1997 for the MOD V8.0 (red), MOD V8.6 (blue) and MOD8.6/GSG (green) total ozone data sets.

and contributes up to ±7 DU depending on its phase while at higher latitudes the eddy heat flux signal (±10 DU) and to lesser extent the ENSO and AO/AAO signals represent the major attribution to ozone variations. The effects of El Chichón (1982) and Mt. Pinatubo (1991) are limited to the periods of volcanic eruptions and are responsible for a large fraction of ozone loss (up to −14 DU and −22 DU, respectively), the signal is more prominent and statistically significant in the Northern Hemisphere.

The signature of the 11-year solar cycle is evident over all latitude bands and the contribution to ozone variability can reach about 13 DU from solar minimum to maximum. Replacing the MgII index by the F10.7 cm proxy, does not change the ozone signal of the other explanatory variables or the statistical significance of the model although the MgII index is believed to correlate better with solar UV irradiance changes than the F10.7 cm solar flux (Viereck et al., 2001, 2004).

Figure 4 shows that the EESC function is the dominant cause of long-term ozone decline in the stratosphere before 1997 and an increase afterwards. The trends are statistically significant in the extratropics and indicates the onset of ozone recovery as expected from the slow decrease in the stratospheric halogen after measures introduced by the Montreal Protocol and amendments to phase out the ODSs. The comparison with trends obtained from the PWLT model yields similar results for the long-term decline before 1997. On the other hand, the positive PWLT turnaround trends are

generally smaller than the EESC trend at southern middle latitudes and have larger uncertainties (the latter due to the shorter periods available for PWLT trends in contrast to the full period used for the EESC trends). The observed ozone changes are as expected from the turnaround in the ODSs since 1997, however, the large year-to-year variability still masks the exact magnitude of the recent (and weak) ODS related trend.

A sensitivity study was carried out by comparing the results obtained from the regression model (Eq. 1) replacing the late MOD V8.6 data after 1995 with the merged GOME/SCIAMACHY/GOME-2 WFDOAS data set (Kiesewetter et al., 2010; Weber et al., 2011, 2013), and with TOMS/SBUV/OMI MOD V8.0 ozone data from 1979 to 2012 (Stolarski and Frith, 2006). This allows us to assess the uncertainty which may arise form the observational data record. Although, some changes in the individual fit parameters were found, within the 2-sigma error bars the results were identical. This is in agreement with an earlier study by Kiesewetter et al. (2010) which also showed a high consistency between the GSG and the merged SBUV V8.6 data. In particular, the EESC related ozone trend is almost identical for the different total ozone data sets, so that the data quality of total ozone data appears to be not an issue here.

The MOD V8.6 data show better agreement of the PWLT with the post-1997 EESC trends, however, the PWLT is for most latitudes are not statistically significantly different from a zero trend. For MOD V8.0 data set, the PWLT trend after 1997 is generally higher than the linear part of the EESC trend but except for the northern subtropics they agree within 2-sigma confidence level.

In summary, the updated trends up to the end of 2012 consolidate the results from other studies (e.g. Mäder et al., 2010) that the observed trend change since 1997 proves the effectiveness of the Montreal Protocol phasing out ODSs. Since the recent ODS decline is fairly slow (Fig. 1), the recent extratropical annual mean total ozone trends are strongly influenced by large year-to-year variability in atmospheric dynamics.

The magnitude of the mostly positive ozone trends observed since 1997 at most latitudes are still somewhat uncertain and, depending on the trend model (EESC or PWLT), may still not be statistically significant different from a zero trend.

**The Supplement related to this article is available online at doi:10.5194/acp-14-7059-2014-supplement.**

## References

Angell, J. K. and Korshover, J.: Quasi-biennial variations in temperature, total ozone, and tropopause height, J. Atmos. Sci., 21, 479–492, 1964.

Appenzeller, C., Weiss, A. K., and Staehelin, J.: North Atlantic Oscillation modulates total ozone winter trends, Geophys. Res. Lett., 27, 1131–1134, 2000.

Aquila, V., Oman, L. D., Stolarski, R., Douglass, A. R., and Newman, P. A.: The Response of Ozone and Nitrogen Dioxide to the Eruption of Mt. Pinatubo at Southern and Northern Midlatitudes, J. Atmos. Sci., 70, 894–900, 2013.

Baldwin, M., Gray, L., Dunkerton, T., Hamilton, K., Haynes, P., Randel, W., Holton, J., Alexander, M., Hirota, I., Horinouchi, T., Jones, D., Kinnersley, J., Marquardt, C., Sato, K., and Takahashi, M.: The Quasi-Biennial Oscillation, Reviews of Geophysics, Rev. Geophys., 39, 179–229, 2001.

Bhartia, P. K., McPeters, R. D., Flynn, L. E., Taylor, S., Kramarova, N. A., Frith, S., Fisher, B., and DeLand, M.: Solar Backscatter UV (SBUV) total ozone and profile algorithm, Atmos. Meas. Tech., 6, 2533–2548, doi:10.5194/amt-6-2533-2013, 2013.

Bojkov, R. D. and Fioletov, V. E.: Estimating the global ozone characteristics during the last 30 years, J. Geophys. Res., 100, 16537–16552, 1995.

Bojkov, R. D., Bishop, L., Hill, W. J., Reinsel, G. C., and Tiao, G. C.: A statistical trend analysis of revised Dobson Total Ozone data over the Northern hemisphere, J. Geophys. Res., 95, 9785–9807, 1990.

Bowman, K. P.: Global patterns of the quasi-biennial oscillation in total ozone, J. Atmos. Sci., 46, 3328–3343, 1989.

Bracher, A., Lamsal, L. N., Weber, M., Bramstedt, K., Coldewey-Egbers, M., and Burrows, J. P.: Global satellite validation of SCIAMACHY $O_3$ columns with GOME WFDOAS, Atmos. Chem. Phys., 5, 2357–2368, doi:10.5194/acp-5-2357-2005, 2005.

Bronnimann, S., Luterbacher, J., Staehelin, J., Svendby, T., Hansen, G., and Svenoe, T.: Extreme climate of the global troposphere and stratosphere in 1940–42 related to El Niño, Nature, 431, 971–974, doi:10.1038/nature02982, 2004.

Camp, C. D. and Tung, K.-K.: Stratospheric polar warming by ENSO in winter: A statistical study, Geophys. Res. Lett., 34, L04809, doi:10.1029/2006GL028521, 2007.

CCMVal, S.: SPARC CCMVal (Stratospheric Processes And their Role in Climate), SPARC Report on the Evaluation of Chemistry-Climate Models, edited by V. Eyring, T.G. Shepherd, and D.W. Waugh, SPARC Report No. 5, WCRP-132, WMO/TD-No. 1526, 478 pp., available at: http://www.atmosp.physics.utoronto.ca/SPARC/ccmval_final/index.php (last access: November 2013), 2010.

Chandra, S. and McPeters, R.: The solar cycle variation of ozone in the stratosphere inferred from NIMBUS7 and NOAA11 satellites, J. Geophys. Res., 99, 20665–20671, 1994.

Chandra, S. and Stolarski, R. S.: Recent trends in stratospheric total ozone: Implications of dynamical and El Chichón perturbations, Geophys. Res. Lett., 18, 2277–2280, 1991.

Chandra, S., Ziemke, J. R., Min, W., and Read, W. G.: Effects of 1997–1998 El Niño on tropospheric ozone and water vapour, Geopshy. Res. Lett., 25, 3867–3870, 1998.

Chandra, S., Ziemke, J. R., Bhartia, P. K., and Martin, R. V.: Tropical tropospheric ozone: Implications for dynamics and biomass burning, J. Geophys. Res., 107, 4188, doi:10.1029/2001JD000447, 2002.

Chipperfield, M. P.: A three-dimensional model study of long-term mid-high latitude lower stratosphere ozone changes, Atmos. Chem. Phys., 3, 1253–1265, doi:10.5194/acp-3-1253-2003, 2003.

Cochrane, D. and Orcutt, G. H.: Application of least squares regression to relationships containing autocorrelated error terms, J. Am. Stat. Assoc., 44, 32–61, 1949.

Coldewey-Egbers, M., Weber, M., Lamsal, L. N., de Beek, R., Buchwitz, M., and Burrows, J. P.: Total ozone retrieval from GOME UV spectral data using the weighting function DOAS approach, Atmos. Chem. Phys., 5, 1015–1025, doi:10.5194/acp-5-1015-2005, 2005.

Daniel, J. S., Solomon, S., and Albritton, D.: On the evaluation of halocarbon radiative forcing and global warming potentials, J. Geophys. Res., 100, 1271–1285, 1995.

DeLand, M. T., Taylor, S. L., Huang, L. K., and Fisher, B. L.: Calibration of the SBUV version 8.6 ozone data product, Atmos. Meas. Tech., 5, 2951–2967, doi:10.5194/amt-5-2951-2012, 2012.

Dhomse, S., Weber, M., Wohltmann, I., Rex, M., and Burrows, J. P.: On the possible causes of recent increases in northern hemispheric total ozone from a statistical analysis of satellite data from 1979 to 2003, Atmos. Chem. Phys., 6, 1165–1180, doi:10.5194/acp-6-1165-2006, 2006.

Dunkerton, T. J. and Baldwin, M. P.: Quasi-biennial modulation of planetary-wave fluxes in the Northern Hemisphere winter, J. Atmos. Sci., 48, 1043–1061, 1991.

Fioletov, V.: Estimating the 27-day and 11-year solar cycle variations in tropical upper stratospheric ozone, J. Geophys. Res., 114, D02302, doi:10.1029/2008JD010499, 2009.

Fioletov, V. E. and Shepherd, T. G.: Seasonal persistence of midlatitude total ozone anomalies, Geophys. Res. Lett., 20, 1417, doi:10.1029/2002GL016739, 2003.

Fioletov, V. E. and Shepherd, T. G.: Summertime total ozone variations over middle and polar latitudes, Geophys. Res. Lett., 32, L04807, doi:10.1029/2004GL022080, 2005.

Fioletov, V. E., Bodeker, G. E., Miller, A. J., McPeters, R. D., and Stolarski, R.: Global and zonal total ozone variations estimated from ground-based and satellite measurements: 1964–2000, J. Geophys. Res.-Atmos., 107, 4647, doi:10.1029/2001jd001350, 2002.

Fioletov, V. E., Labow, G., Evans, R., Hare, E. W., Köhler, U., McElroy, C. T., Miyagawa, K., Redondas, A., Savastiouk, V., Shalamyansky, A. M., Staehelin, J., Vanicek, K., and Weber, M.: The performance of the ground-based total ozone network assessed using satellite data, J. Geophys. Res., 113, D14313, doi:10.1029/2008JD009809, 2008.

Frith, S., McPeters, R., Kramarova, N., Bhartia, P. K., Labow, G., Stolarski, R., Taylor, S., Fisher, B., and DeLand, M.: A 40-year Record of Profile Ozone from the SBUV(/2) Instrument Series, Guadrennial Ozone Symposium 2012, Toronto, Canada, 26–31 August, 2012, 2012.

Frossard, L., Rieder, H. E., Ribatet, M., Staehelin, J., Maeder, J. A., Di Rocco, S., Davison, A. C., and Peter, T.: On the relationship between total ozone and atmospheric dynamics and chemistry at midlatitudes – Part 1: Statistical models and spatial fingerprints of atmospheric dynamics and chemistry, Atmos. Chem. Phys., 13, 147–164, doi:10.5194/acp-13-147-2013, 2013.

Fujiwara, M., Kita, K., Kawakami, S., Ogawa, T., Komala, N., Saraspriya, S., and Suripto, A.: Tropospheric ozone enhancements during the Indonesian forest fire events in 1994 and in 1997 as revealed by ground-based observations, Geophys. Res. Lett., 26, 2417–2420, doi:10.1029/1999GL900117, 1999.

Fusco, A. C. and Salby, M. L.: Interannual variations of total ozone and their relationship to variations of planetary wave activity, J. Climate, 12, 1619–1629, 1999.

Harris, N. R. P., Kyrö, E., Staehelin, J., Brunner, D., Andersen, S.-B., Godin-Beekmann, S., Dhomse, S., Hadjinicolaou, P., Hansen, G., Isaksen, I., Jrrar, A., Karpetchko, A., Kivi, R., Knudsen, B., Krizan, P., Lastovicka, J., Maeder, J., Orsolini, Y., Pyle, J. A., Rex, M., Vanicek, K., Weber, M., Wohltmann, I., Zanis, P., and Zerefos, C.: Ozone trends at northern mid- and high latitudes – a European perspective, Ann. Geophys., 26, 1207–1220, doi:10.5194/angeo-26-1207-2008, 2008.

Hartmann, D. L., M.Wallace, J., Limpasuvan, V., Thompson, D., and Holton, J. R.: Can ozone depletion and global warming interact to produce rapid climate change?, P. Natl. Acad. Sci. USA, 97, 1412–1417, 2000.

Haynes, P. H., Marks, C. J., McIntyre, M. E., Shepherd, T. G., and Shine, K. P.: On the "downward control" of extratropical diabatic circulations by eddy-induced mean zonal forces, J. Atmos. Sci., 48, 651–678, 1991.

Hofmann, D. J. and Solomon, S.: Ozone destruction through heterogeneous chemistry following the eruption of El Chichón, J. Geophys. Res., 94, 5029–5041, 1989.

Holton, J. R. and Tan, H.-C.: The influence of the equatorial quasi-biennial oscillation on the global circulation at 50 mb, J. Atmos. Sci., 37, 2200–2208, 1980.

Hood, L. L.: The solar cycle variation of total ozone: Dynamical forcing in the lower stratosphere, J. Geophys. Res., 102, 1355–1370, 1997.

Hood, L. L. and Soukharev, B. E.: Interannual variations of total ozone at northern midlatitudes correlated with stratospheric EP flux and potential vorticity, J. Atmos. Sci., 62, 3724–3740, 2005.

Kiesewetter, G., Sinnhuber, B.-M., Weber, M., and Burrows, J. P.: Attribution of stratospheric ozone trends to chemistry and transport: a modelling study, Atmos. Chem. Phys., 10, 12073–12089, doi:10.5194/acp-10-12073-2010, 2010.

Koukouli, M. E., Balis, D. S., Loyola, D., Valks, P., Zimmer, W., Hao, N., Lambert, J.-C., Van Roozendael, M., Lerot, C., and Spurr, R. J. D.: Geophysical validation and long-term consistency between GOME-2/MetOp-A total ozone column and measurements from the sensors GOME/ERS-2, SCIA-MACHY/ENVISAT and OMI/Aura, Atmos. Meas. Tech., 5, 2169–2181, doi:10.5194/amt-5-2169-2012, 2012.

Labitzke, K. and van Loon, H.: The Stratosphere, Springer-Verlag, New York, p. 179 pp., 1999.

Lait, L. R., Schoeberl, M. R., and Newman, P. A.: Quasibiennial modulation of the Antarctic ozone depletion, J. Geophys. Res., 94, 11559–11571, 1989.

Lee, H. and Smith, A.: Simulation of the combined effects of solar cycle, quasi-biennial oscillation, and volcanic forcing on stratospheric ozone changes in recent decades, J. Geophys. Res., 108, 4049, doi:10.1029/2001JD001503, 2003.

Lerot, C., Van Roozendael, M., Spurr, R., Loyola, D., Coldewey-Egbers, M., Kochenova, S., van Gent, J., Koukouli, M., Balis, D., Lambert, J.-C., Granville, J., and Zehner, C.: Homogenized total ozone data records from the European sensors GOME/ERS-2, SCIAMACHY/Envisat and GOME-2/MetOp-A, J. Geophys. Res., 119, 1639–1662, doi:10.1002/2013JD020831, 2013.

Loyola, D. and Coldewey-Egbers, M.: Multi-sensor data merging with stacked neural networks for the creation of satellite long-term climate data records, EURASIP J. Adv. Sig. Pr., 2012, 1–10, doi:10.1186/1687-6180-2012-91, 2012.

Mäder, J. A., Staehelin, J., Brunner, D., Stahel, W. A., Wohltmann, I., and Peter, T.: Statistical modeling of total ozone: selection of appropriate explanatory variables, J. Geophys. Res. Atmos, 112, D11108, doi:10.1029/2006jd007694, 2007.

Mäder, J. A., Staehelin, J., Peter, T., Brunner, D., Rieder, H. E., and Stahel, W. A.: Evidence for the effectiveness of the Montreal Protocol to protect the ozone layer, Atmos. Chem. Phys., 10, 12161–12171, doi:10.5194/acp-10-12161-2010, 2010.

Manzini, E., Giorgetta, M. A., Esch, M., Kornblueh, L., and Roeckner, E.: The influence of sea surface temperatures on the northern winter stratosphere: Ensemble simulations with the MAECHAM5 model, J. Climate, 19, 3863–3881, doi:10.1175/JCLI3826.1, 2006.

McCormack, J. P., Hood, L. L., Nagatani, R., Miller, A. J., Planet, W. G., and McPeters, R. D.: Approximate separation of volcanic and 11-year signals in the SBUV-SBUV/2 total ozone record over the 1979–1995 period, Geophys. Res. Lett., 24, 2729–2732, 1997.

McPeters, R. D., Bhartia, P. K., Haffner, D., Labow, G. J., and Flynn, L.: The version 8.6 SBUV ozone data record: An overview, J. Geophys. Res.-Atmos., 118, 8032–8039, doi:10.1002/jgrd.50597, 2013.

Miller, A., Cai, A., Taio, G., Wuebbles, D., Flynn, L., Yang, S.-K., Weatherhead, E., Fioletov, V., Petropavlovskikh, I., Meng, X.-L., Guillas, S., Nagatani, R., and Reinsel, G.: Examination of ozonesonde data for trends and trend changes incorporating solar and Arctic oscillation signals, J. Geophys. Res., 111, D13305, doi:10.1029/2005JD006684, 2006.

Miller, A. J., Hollandsworth, S. M., Flynn, L. E., Tiao, G. C., Reinsel, G. C., Bishop, L., McPeters, R. D., Planet, W. G., DeLuisi, J. J., Mateer, C. L., Wuebbles, D., Kerr, J., and Nagatani, R. M.: Comparisons of observed ozone trends and solar effects in the stratosphere through examination of ground-based Umkehr and combined solar backscattered ultraviolet (SBUV) and SBUV 2 satellite data, J. Geophys. Res., 101, 9017–9021, 1996.

Nair, P. J., Godin-Beekmann, S., Kuttippurath, J., Ancellet, G., Goutail, F., Pazmiño, A., Froidevaux, L., Zawodny, J. M., Evans, R. D., Wang, H. J., Anderson, J., and Pastel, M.: Ozone trends derived from the total column and vertical profiles at a northern midlatitude station, Atmos. Chem. Phys., 13, 10373–10384, doi:10.5194/acp-13-10373-2013, 2013.

Newchurch, M. J., Yang, E.-S., Cunnold, D. M., Reinsel, G. C., and. Zawodny, J. M., and Russell, J. M.: Evidence for slowdown in stratospheric ozone loss: First stage of ozone recovery, J. Geophys. Res., 108, 4507, doi:10.1029/2003JD003471, 2003.

Newman, P. A., Nash, E. R., and Rosenfield, J. E.: What controls the temperature of the arctic stratosphere during the spring?, J. Geophys. Res., 106, 19999–20010, 2001.

Newman, P. A., Kawa, S. R., and Nash, E. R.: On the size of the Antarctic ozone hole, Geophys. Res. Lett., 31, L21104, doi:10.1029/2004GL020596, 2004.

Newman, P. A., Nash, E. R., Kawa, S. R., Montzka, S. A., and Schauffler, S. M.: When will the Antarctic ozone hole recover?, Geophys. Res. Lett., 33, L12814, doi:10.1029/2005GL025232, 2006.

Newman, P. A., Daniel, J. S., Waugh, D. W., and Nash, E. R.: A new formulation of equivalent effective stratospheric chlorine (EESC), Atmos. Chem. Phys., 7, 4537–4552, doi:10.5194/acp-7-4537-2007, 2007.

Peter, T.: Microphysics and heterogeneous chemistry of polar stratospheric clouds, Annu. Rev. Phys. Chem., 48, 785–822, 1997.

Plumb, R. A.: Stratospheric transport, J. Meteor. Soc. Jpn., 80, 793–809, 2002.

Randel, W. J. and Wu, F.: A stratospheric ozone profile data set for 1979–2005: Variability, trends, and comparisons with column ozone data, J. Geophys. Res., 112, D06313, doi:10.1029/2006JD007339, 2007.

Randel, W. J. and Wu, F. and Stolarski, R.: Changes in column ozone correlated with the stratospheric EP flux, J. Meteorol. Soc. Jpn., 80, 849–862, 2002.

Randel, W. J. and Cobb, J. B.: Coherent variations of monthly mean column ozone and lower stratospheric temperature, J. Geophys. Res., 99, 5433–5447, 1994.

Randel, W. J., Wu, F., Russell III, J. M., Waters, J. W., and Froidevaux, L.: Ozone and temperature changes in the stratosphere following the eruption of Mt. Pinatubo, J. Geophys. Res., 100, 16753–16764, 1995.

Reinsel, G. C., Weatherhead, E. C., Tiao, G. C., Miller, A. J., Nagatani, R. M., Wuebbles, D. J., and Flynn, L. E.: On detection of turnaround and recovery in trend for ozone, J. Geophys. Res., 107, 4078, doi:10.1029/2001JD000500, 2002.

Reinsel, G. C., Miller, A. J., Weatherhead, E. C., Flynn, L. E., Nagatani, R. M., Tiao, G. C., and Wuebbles, D. J.: Trend analysis of total ozone data for turnaround and dynamical contributions, J. Geophys. Res., 110, D16306, doi:10.1029/2004JD004662, 2005.

Rieder, H. E., Staehelin, J., Maeder, J. A., Peter, T., Ribatet, M., Davison, A. C., Stübi, R., Weihs, P., and Holawe, F.: Extreme events in total ozone over Arosa – Part 1: Application of extreme value theory, Atmos. Chem. Phys., 10, 10021–10031, doi:10.5194/acp-10-10021-2010, 2010a.

Rieder, H. E., Staehelin, J., Maeder, J. A., Peter, T., Ribatet, M., Davison, A. C., Stübi, R., Weihs, P., and Holawe, F.: Extreme events in total ozone over Arosa – Part 2: Fingerprints of atmospheric dynamics and chemistry and effects on mean values and long-term changes, Atmos. Chem. Phys., 10, 10033–10045, doi:10.5194/acp-10-10033-2010, 2010b.

Rieder, H. E., Jancso, L. M., Di Rocco, S., Staehelin, J., Mäder, J. A., Peter, T., Ribatet, M., Davison, A. C., De Backer, H., Koehler, U., Krzyścin, J., and Vaniček, K.: Extreme events in

total ozone over the northern midlatitudes: an analysis based on long-term data sets from five European ground-based stations, Tellus B, North America, 63, 860–874, doi:10.1111/j.1600-0889.2011.00575.x, 2011.

Rieder, H. E., Frossard, L., Ribatet, M., Staehelin, J., Maeder, J. A., Di Rocco, S., Davison, A. C., Peter, T., Weihs, P., and Holawe, F.: On the relationship between total ozone and atmospheric dynamics and chemistry at midlatitudes – Part 2: The effects of the El Niño/Southern Oscillation, volcanic eruptions and contributions of atmospheric dynamics and chemistry to long-term total ozone changes, Atmos. Chem. Phys., 13, 165–179, doi:10.5194/acp-13-165-2013, 2013.

Rosenlof, K. and Holton, J. R.: Estimates of the stratospheric residual circulation using the downward control principle, J. Geophys. Res., 98, 10465–10479, 1993.

Sato, M., Hansen, J. E., McCormack, M. P., and Pollack, J. B.: Stratospheric aerosol optical depth, J. Geophys. Res., 98, 1850–1990, 1993.

Schnadt Poberaj, C., Staehelin, J., and Brunner, D.: Missing stratospheric ozone decrease at Southern Hemisphere middle latitudes after Mt. Pinatubo: a dynamical perspective, J. Atmos. Sci., 68, 1922–1945, 2011.

Sinnhuber, B.-M., Sheode, N., Sinnhuber, M., Chipperfield, M. P., and Feng, W.: The contribution of anthropogenic bromine emissions to past stratospheric ozone trends: a modelling study, Atmos. Chem. Phys., 9, 2863–2871, doi:10.5194/acp-9-2863-2009, 2009.

Solomon, S.: Stratospheric ozone depletion: a review of concepts and history, Rev. Geophys., 37, 275–316, 1999.

Solomon, S., Portman, R. W., Garcia, R. R., Thomason, L. W., Poole, L. R., and McCormack, M. P.: The role of aerosol variations in anthropogenic ozone depletion at northern midlatitudes, J. Geophys. Res., 101, 6713–6727, 1996.

Soukharev, B. and Hood, L.: Solar cycle variation of stratospheric ozone: Multiple regression analysis of long-term satellite data sets and comparisons with models, J. Geophys. Res., 111, D20314, doi:10.1029/2006JD007107, 2006.

SPARC: Stratospheric Processes And their Role in Climate: Assessment of trends in the vertical distribution of ozone, SPARC Report 1, edited by: Harris, N., Hudson, R., and Phillips, C., SPARC Report No. 1, 1998.

Staehelin, J., Kegel, R., and Harris, N. R. P.: rend analysis of the homogenized total ozone series of Arosa (Switzerland), 1926–1996, J. Geophys. Res.-Atmos., 103, 8389–8399, 1998.

Staehelin, J., Harris, N. R. P., Appenzeller, C., and Eberhard, J.: Ozone trends: A review, Rev. Geophys., 39, 231–290, 2001.

Steinbrecht, W., Hassler, B., Claude, H., Winkler, P., and Stolarski, R. S.: Global distribution of total ozone and lower stratospheric temperature variations, Atmos. Chem. Phys., 3, 1421–1438, doi:10.5194/acp-3-1421-2003, 2003.

Steinbrecht, W., Koehler, U., Claude, H., Weber, M., Burrows, J. P., and van der A, R. J.: Very high ozone columns at northern midlatitudes in 2010, Geophys. Res. Lett., 38, L06803, doi:10.1029/2010GL046634, 2011.

Stolarski, R. S. and Frith, S. M.: Search for evidence of trend slowdown in the long-term TOMS/SBUV total ozone data record: the importance of instrument drift uncertainty, Atmos. Chem. Phys., 6, 4057–4065, doi:10.5194/acp-6-4057-2006, 2006.

Sudo, K. and Takahashi, M.: Simulation of tropospheric ozone changes during 1997–1998 El Niño: Meteorological impact on tropospheric photochemistry, Geophys. Res. Lett., 23, 4091–4094, 2001.

Taguchi, M. and Hartmann, D. L.: Increased occurrence of stratospheric sudden warming during El Niño as simulated by WACCM, J. Climate, 19, 324–332, 2006.

Thompson, A. M., Witte, J. C., Hudson, R. D., Guo, H., Herman, J. R., and Fujiwara, M.: Tropical tropospheric ozone and biomass burning, Science, 291, 2128–2132, 2001.

Trenberth, K. E., Caron, J. M., Stepaniak, D. P., and Worley, S.: Evolution of El Niño – Southern Oscillation and global atmospheric surface temperatures, J. Geophys. Res., 107, 4065, doi:10.1029/2000JD000298, 2002.

Tung, K. and Yang, H.: Global QBO in circulation and ozone, part I, Reexamination of observational evidence, J. Atmos. Sci., 51, 2699–2707, 1994.

van Loon, H. and Labitzke, K.: The Southern Oscillation. Part V: The anomalies in the lower stratosphere of the Northern Hemisphere in winter and a comparison with the Quasi–Biennial Oscillation, Mon. Weather Rev., 115, 357–369, 1987.

Van Roozendael, M., Loyola, D., Spurr, R., Balis, D., Lambert, J. C., Livschitz, Y., Valks, P., Ruppert, T., Kenter, P., Fayt, C., and Zehner, C.: Ten years of GOME/ERS-2 total ozone data: the new GOME Data Processor (GDP) version 4: Algorithm Description, J. Geophys. Res., 111, D14311, doi:10.1029/2005JD006375, 2006.

Viereck, R. A., Puga, L., McMullin, D., Judge, D., Weber, M., and Tobiska, W. K.: The Mg II index: A proxy for solar EUV, Geophys. Res. Lett., 28, 1343–1346, 2001.

Viereck, R. A., Floyd, L. E., Crane, P. C., Woods, T. N., Knapp, B. G., Rottman, G., Weber, M., Puga, L. C., and DeLand, M. T.: A composite Mg IIindex spanning from 1978 to 2003, Space Weather, 2, S10005, doi:10.1029/2004SW000084, 2004.

Vyushin, D., Fioletov, V., and Shepherd, T.: Impact of long-range correlations on trend detection in total ozone, J. Geophys. Res., 112, D14307, doi:10.1029/2006JD008168, 2007.

Vyushin, D., Shepherd, T., and Fioletov, V.: On the statistical modeling of persistence in total ozone anomalies, J. Geophys. Res., 115, D16306, doi:10.1029/2009JD013105, 2010.

Weber, M., Lamsal, L. N., Coldewey-Egbers, M., Bramstedt, K., and Burrows, J. P.: Pole-to-pole validation of GOME WFDOAS total ozone with groundbased data, Atmos. Chem. Phys., 5, 1341–1355, doi:10.5194/acp-5-1341-2005, 2005.

Weber, M., Lamsal, L. N., and Burrows, J. P.: Improved SCIAMACHY WFDOAS total ozone retrieval: steps towards homogenising long-term total ozone datasets from GOME, SCIAMACHY, and GOME2, Proc. 'Envisat Symposium 2007', Montreux, Switzerland, 23-27 April 2007, ESA SP-636, July 2007, available at: http://envisat.esa.int/envisatsymposium/proceedings/posters/3P4/463281we.pdf (last access: November 2013), 2007.

Weber, M., Dikty, S., Burrows, J. P., Garny, H., Dameris, M., Kubin, A., Abalichin, J., and Langematz, U.: The Brewer-Dobson circulation and total ozone from seasonal to decadal time scales, Atmos. Chem. Phys., 11, 11221–11235, doi:10.5194/acp-11-11221-2011, 2011.

Weber, M., Chehade, W., Fioletov, V. E., Frith, S. M., Long, C. S., Steinbrecht, W., and Wild, J. D.: Stratospheric Ozone,

in: State of the Climate in 2012, edited by: Blunden, J. and Arndt, D. S., B. Am. Meteorol. Soc., 94, S36–S37, doi:10.1175/2013BAMSStateoftheClimate.1, 2013.

WMO: World Meteorological Organization: Global Ozone Research and Monitoring Project.Scientific Assessment of Ozone Depletion: 1998, Report No. 44, World Meteorological Organization, Geneva, 1999.

WMO: World Meteorological Organization: Global Ozone Research and Monitoring Project.Scientific Assessment of Ozone Depletion: 2002, Report No. 47, World Meteorological Organization, Geneva, 2003.

WMO: World Meteorological Organization: Global Ozone Research and Monitoring Project.Scientific Assessment of Ozone Depletion: 2006, Report No. 50, World Meteorological Organization, Geneva, 2007.

WMO: World Meteorological Organization: Global Ozone Research and Monitoring Project.Scientific Assessment of Ozone Depletion: 2010, Report No. 52, World Meteorological Organization, Geneva, 2011.

Wohltmann, I., Lehmann, R., Rex, M., Brunner, D., and Mäder, J. A.: A process-oriented regression model for column ozone, J. Geophys. Res.-Atmos., 112, D12304, doi:10.1029/2006jd007573, 2007.

Yang, S.-K., Long, C., Miller, A., He, X., Yang, Y., Wuebbles, D., and Tiao, G.: Modulation of natural variability on a trend analysis of updated cohesive SBUV(/2) total ozone, Int. J. Remote Sens., 30, 3975–3986, doi:10.1080/01431160902821924, 2009.

Zeng, G. and Pyle, J. A.: Influence of El Niño Southern Oscillation on stratosphere/troposphere exchange and the global tropospheric ozone budget, Geophys. Res. Lett., 32, L0814, doi:10.1020/2004GL021353, 2005.

Zerefos, C. S., Tourpali, K., Bojkov, R., Balis, D., Rognerund, B., and Isaksen, I.: Solar acticity – total ozone relationships: observations and model studies with heterogeneous chemistry, J. Geophys. Res., 102, 1561–1569, 1997.

Ziemke, J. R. and Chandra, S.: Development of a climate record of tropospheric and stratospheric column ozone from satellite remote sensing: evidence of an early recovery of global stratospheric ozone, Atmos. Chem. Phys., 12, 5737–5753, doi:10.5194/acp-12-5737-2012, 2012.

Ziemke, J. R., Chandra, S., McPeters, R. D., and Newman, P. A.: Dynamical proxies of column ozone with applications to global trend models, J. Geophys. Res., 102, 6117–6129, 1997.

Ziemke, J. R., Chandra, S., Oman, L. D., and Bhartia, P. K.: A new ENSO index derived from satellite measurements of column ozone, Atmos. Chem. Phys., 10, 3711–3721, doi:10.5194/acp-10-3711-2010, 2010.